PHYSICAL REVIEW LETTERS

Measurement of the Ratios of Branching Fractions $\mathcal{B}(B_s^0 \to D_s^- \pi^+)/\mathcal{B}(B^0 \to D^- \pi^+)$ and $\mathcal{B}(B^+ \to \bar{D}^0 \pi^+)/\mathcal{B}(B^0 \to D^- \pi^+)$

A. Abulencia,[23] D. Acosta,[17] J. Adelman,[13] T. Affolder,[10] T. Akimoto,[53] M. G. Albrow,[16] D. Ambrose,[16] S. Amerio,[42] D. Amidei,[33] A. Anastassov,[50] K. Anikeev,[16] A. Annovi,[44] J. Antos,[1] M. Aoki,[53] G. Apollinari,[16] J.-F. Arguin,[32] T. Arisawa,[55] A. Artikov,[14] W. Ashmanskas,[16] A. Attal,[8] F. Azfar,[41] P. Azzi-Bacchetta,[42] P. Azzurri,[44] N. Bacchetta,[42] H. Bachacou,[28] W. Badgett,[16] A. Barbaro-Galtieri,[28] V. E. Barnes,[46] B. A. Barnett,[24] S. Baroiant,[7] V. Bartsch,[30] G. Bauer,[31] F. Bedeschi,[44] S. Behari,[24] S. Belforte,[52] G. Bellettini,[44] J. Bellinger,[57] A. Belloni,[31] E. Ben-Haim,[16] D. Benjamin,[15] A. Beretvas,[16] J. Beringer,[28] T. Berry,[29] A. Bhatti,[48] M. Binkley,[16] D. Bisello,[42] M. Bishai,[16] R. E. Blair,[2] C. Blocker,[6] K. Bloom,[33] B. Blumenfeld,[24] A. Bocci,[48] A. Bodek,[47] V. Boisvert,[47] G. Bolla,[46] A. Bolshov,[31] D. Bortoletto,[46] J. Boudreau,[45] S. Bourov,[16] A. Boveia,[10] B. Brau,[10] C. Bromberg,[34] E. Brubaker,[13] J. Budagov,[14] H. S. Budd,[47] S. Budd,[23] K. Burkett,[16] G. Busetto,[42] P. Bussey,[20] K. L. Byrum,[2] S. Cabrera,[15] M. Campanelli,[19] M. Campbell,[33] F. Canelli,[8] A. Canepa,[46] D. Carlsmith,[57] R. Carosi,[44] S. Carron,[15] M. Casarsa,[52] A. Castro,[5] P. Catastini,[44] D. Cauz,[52] M. Cavalli-Sforza,[3] A. Cerri,[28] L. Cerrito,[41] S. H. Chang,[27] J. Chapman,[33] Y. C. Chen,[1] M. Chertok,[7] G. Chiarelli,[44] G. Chlachidze,[14] F. Chlebana,[16] I. Cho,[27] K. Cho,[27] D. Chokheli,[14] J. P. Chou,[21] P. H. Chu,[23] S. H. Chuang,[57] K. Chung,[12] W. H. Chung,[57] Y. S. Chung,[47] M. Ciljak,[44] C. I. Ciobanu,[23] M. A. Ciocci,[44] A. Clark,[19] D. Clark,[6] M. Coca,[15] A. Connolly,[28] M. E. Convery,[48] J. Conway,[7] B. Cooper,[30] K. Copic,[33] M. Cordelli,[18] G. Cortiana,[42] A. Cruz,[17] J. Cuevas,[11] R. Culbertson,[16] D. Cyr,[57] S. DaRonco,[42] S. D'Auria,[20] M. D'onofrio,[19] D. Dagenhart,[6] P. de Barbaro,[47] S. De Cecco,[49] A. Deisher,[28] G. De Lentdecker,[47] M. Dell'Orso,[44] S. Demers,[47] L. Demortier,[48] J. Deng,[15] M. Deninno,[5] D. De Pedis,[49] P. F. Derwent,[16] C. Dionisi,[49] J. Dittmann,[4] P. DiTuro,[50] C. Dörr,[25] A. Dominguez,[28] S. Donati,[44] M. Donega,[19] P. Dong,[8] J. Donini,[42] T. Dorigo,[42] S. Dube,[50] K. Ebina,[55] J. Efron,[38] J. Ehlers,[19] R. Erbacher,[7] D. Errede,[23] S. Errede,[23] R. Eusebi,[47] H. C. Fang,[28] S. Farrington,[29] I. Fedorko,[44] W. T. Fedorko,[13] R. G. Feild,[58] M. Feindt,[25] J. P. Fernandez,[46] R. Field,[17] G. Flanagan,[34] L. R. Flores-Castillo,[45] A. Foland,[21] S. Forrester,[7] G. W. Foster,[16] M. Franklin,[21] J. C. Freeman,[28] Y. Fujii,[26] I. Furic,[13] A. Gajjar,[29] M. Gallinaro,[48] J. Galyardt,[12] J. E. Garcia,[44] M. Garcia Sciverez,[28] A. F. Garfinkel,[46] C. Gay,[58] H. Gerberich,[23] E. Gerchtein,[12] D. Gerdes,[33] S. Giagu,[49] P. Giannetti,[44] A. Gibson,[28] K. Gibson,[12] C. Ginsburg,[16] K. Giolo,[46] M. Giordani,[52] M. Giunta,[44] G. Giurgiu,[12] V. Glagolev,[14] D. Glenzinski,[16] M. Gold,[36] N. Goldschmidt,[33] J. Goldstein,[41] G. Gomez,[11] G. Gomez-Ceballos,[11] M. Goncharov,[51] O. González,[46] I. Gorelov,[36] A. T. Goshaw,[15] Y. Gotra,[45] K. Goulianos,[48] A. Gresele,[42] M. Griffiths,[29] S. Grinstein,[21] C. Grosso-Pilcher,[13] U. Grundler,[23] J. Guimaraes da Costa,[21] C. Haber,[28] S. R. Hahn,[16] K. Hahn,[43] E. Halkiadakis,[47] A. Hamilton,[32] B-Y. Han,[47] R. Handler,[57] F. Happacher,[18] K. Hara,[53] M. Hare,[54] S. Harper,[41] R. F. Harr,[56] R. M. Harris,[16] K. Hatakeyama,[48] J. Hauser,[8] C. Hays,[15] H. Hayward,[29] A. Heijboer,[43] B. Heinemann,[29] J. Heinrich,[43] M. Hennecke,[25] M. Herndon,[57] J. Heuser,[25] D. Hidas,[15] C. S. Hill,[10] D. Hirschbuehl,[25] A. Hocker,[16] A. Holloway,[21] S. Hou,[1] M. Houlden,[29] S.-C. Hsu,[9] B. T. Huffman,[41] R. E. Hughes,[38] J. Huston,[34] K. Ikado,[55] J. Incandela,[10] G. Introzzi,[44] M. Iori,[49] Y. Ishizawa,[53] A. Ivanov,[7] B. Iyutin,[31] E. James,[16] D. Jang,[50] B. Jayatilaka,[33] D. Jeans,[49] H. Jensen,[16] E. J. Jeon,[27] M. Jones,[46] K. K. Joo,[27] S. Y. Jun,[12] T. R. Junk,[23] T. Kamon,[51] J. Kang,[33] M. Karagoz-Unel,[37] P. E. Karchin,[56] Y. Kato,[40] Y. Kemp,[25] R. Kephart,[16] U. Kerzel,[25] V. Khotilovich,[51] B. Kilminster,[38] D. H. Kim,[27] H. S. Kim,[27] J. E. Kim,[27] M. J. Kim,[12] M. S. Kim,[27] S. B. Kim,[27] S. H. Kim,[53] Y. K. Kim,[13] M. Kirby,[15] L. Kirsch,[6] S. Klimenko,[17] M. Klute,[31] B. Knuteson,[31] B. R. Ko,[15] H. Kobayashi,[53] K. Kondo,[55] D. J. Kong,[27] J. Konigsberg,[17] A. Korytov,[17] A. V. Kotwal,[15] A. Kovalev,[43] J. Kraus,[23] I. Kravchenko,[31] M. Kreps,[25] A. Kreymer,[16] J. Kroll,[43] N. Krumnack,[4] M. Kruse,[15] V. Krutelyov,[51] S. E. Kuhlmann,[2] Y. Kusakabe,[55] S. Kwang,[13] A. T. Laasanen,[46] S. Lai,[32] S. Lami,[48] S. Lami,[48] S. Lammel,[16] M. Lancaster,[30] R. L. Lander,[7] K. Lannon,[38] A. Lath,[50] G. Latino,[44] I. Lazzizzera,[42] C. Lecci,[25] T. LeCompte,[2] J. Lee,[47] J. Lee,[47] S. W. Lee,[51] R. Lefèvre,[3] N. Leonardo,[31] S. Leone,[44] S. Levy,[13] J. D. Lewis,[16] K. Li,[58] C. Lin,[58] C. S. Lin,[16] M. Lindgren,[16] E. Lipeles,[9] T. M. Liss,[23] A. Lister,[19] D. O. Litvintsev,[16] T. Liu,[16] Y. Liu,[19] N. S. Lockyer,[43] A. Loginov,[35] M. Loreti,[42] P. Loverre,[49] R.-S. Lu,[1] D. Lucchesi,[42] P. Lujan,[28] P. Lukens,[16] G. Lungu,[17] L. Lyons,[41] J. Lys,[28] R. Lysak,[1] E. Lytken,[46] P. Mack,[25] D. MacQueen,[32] R. Madrak,[16] K. Maeshima,[16] P. Maksimovic,[24] G. Manca,[29] F. Margaroli,[5] R. Marginean,[16] C. Marino,[23] A. Martin,[58] M. Martin,[24] V. Martin,[37] M. Martínez,[3] T. Maruyama,[53] H. Matsunaga,[53] M. E. Mattson,[56] R. Mazini,[32] P. Mazzanti,[5] K. S. McFarland,[47] D. McGivern,[30] P. McIntyre,[51] P. McNamara,[50] R. McNulty,[29] A. Mehta,[29] S. Menzemer,[31] A. Menzione,[44] P. Merkel,[46] C. Mesropian,[48] A. Messina,[49] M. von der Mey,[8] T. Miao,[16] N. Miladinovic,[6] J. Miles,[31] R. Miller,[34] J. S. Miller,[33] C. Mills,[10] M. Milnik,[25] R. Miquel,[28] S. Miscetti,[18] G. Mitselmakher,[17] A. Miyamoto,[26] N. Moggi,[5] B. Mohr,[8] R. Moore,[16] M. Morello,[44] P. Movilla Fernandez,[28] J. Mülmenstädt,[28]

191801-1

A. Mukherjee,[16] M. Mulhearn,[31] Th. Muller,[25] R. Mumford,[24] P. Murat,[16] J. Nachtman,[16] S. Nahn,[58] I. Nakano,[39] A. Napier,[54] D. Naumov,[36] V. Necula,[17] C. Neu,[43] M. S. Neubauer,[9] J. Nielsen,[28] T. Nigmanov,[45] L. Nodulman,[2] O. Norniella,[3] T. Ogawa,[55] S. H. Oh,[15] Y. D. Oh,[27] T. Okusawa,[40] R. Oldeman,[29] R. Orava,[22] K. Osterberg,[22] C. Pagliarone,[44] E. Palencia,[11] R. Paoletti,[44] V. Papadimitriou,[16] A. Papikonomou,[25] A. A. Paramonov,[13] B. Parks,[38] S. Pashapour,[32] J. Patrick,[16] G. Pauletta,[52] M. Paulini,[12] C. Paus,[31] D. E. Pellett,[7] A. Penzo,[52] T. J. Phillips,[15] G. Piacentino,[44] J. Piedra,[11] K. Pitts,[23] C. Plager,[8] L. Pondrom,[57] G. Pope,[45] X. Portell,[3] O. Poukhov,[14] N. Pounder,[41] F. Prakoshyn,[14] A. Pronko,[16] J. Proudfoot,[2] F. Ptohos,[18] G. Punzi,[44] J. Pursley,[24] J. Rademacker,[41] A. Rahaman,[45] A. Rakitin,[31] S. Rappoccio,[21] F. Ratnikov,[50] B. Reisert,[16] V. Rekovic,[36] N. van Remortel,[22] P. Renton,[41] M. Rescigno,[49] S. Richter,[25] F. Rimondi,[5] K. Rinnert,[25] L. Ristori,[44] W. J. Robertson,[15] A. Robson,[20] T. Rodrigo,[11] E. Rogers,[23] S. Rolli,[54] R. Roser,[16] M. Rossi,[52] R. Rossin,[17] C. Rott,[46] A. Ruiz,[11] J. Russ,[12] V. Rusu,[13] D. Ryan,[54] H. Saarikko,[22] S. Sabik,[32] A. Safonov,[7] W. K. Sakumoto,[47] G. Salamanna,[49] O. Salto,[3] D. Saltzberg,[8] C. Sanchez,[3] L. Santi,[52] S. Sarkar,[49] K. Sato,[53] P. Savard,[32] A. Savoy-Navarro,[16] T. Scheidle,[25] P. Schlabach,[16] E. E. Schmidt,[16] M. P. Schmidt,[58] M. Schmitt,[37] T. Schwarz,[33] L. Scodellaro,[11] A. L. Scott,[10] A. Scribano,[44] F. Scuri,[44] A. Sedov,[46] S. Seidel,[36] Y. Seiya,[40] A. Semenov,[14] F. Semeria,[5] L. Sexton-Kennedy,[16] I. Sfiligoi,[18] M. D. Shapiro,[28] T. Shears,[29] P. F. Shepard,[45] D. Sherman,[21] M. Shimojima,[53] M. Shochet,[13] Y. Shon,[57] I. Shreyber,[35] A. Sidoti,[44] P. Sinervo,[32] A. Sisakyan,[14] J. Sjolin,[41] A. Skiba,[25] A. J. Slaughter,[16] K. Sliwa,[54] D. Smirnov,[36] J. R. Smith,[7] F. D. Snider,[16] R. Snihur,[32] M. Soderberg,[33] A. Soha,[7] S. Somalwar,[50] V. Sorin,[34] J. Spalding,[16] F. Spinella,[44] P. Squillacioti,[44] M. Stanitzki,[58] A. Staveris-Polykalas,[44] R. St. Denis,[20] B. Stelzer,[8] O. Stelzer-Chilton,[32] D. Stentz,[37] J. Strologas,[36] D. Stuart,[10] J. S. Suh,[27] A. Sukhanov,[17] K. Sumorok,[31] H. Sun,[54] T. Suzuki,[53] A. Taffard,[23] R. Tafirout,[32] R. Takashima,[39] Y. Takeuchi,[53] K. Takikawa,[53] M. Tanaka,[2] R. Tanaka,[39] M. Tecchio,[33] P. K. Teng,[1] K. Terashi,[48] S. Tether,[31] J. Thom,[16] A. S. Thompson,[20] E. Thomson,[43] P. Tipton,[47] V. Tiwari,[12] S. Tkaczyk,[16] D. Toback,[51] K. Tollefson,[34] T. Tomura,[53] D. Tonelli,[44] M. Tönnesmann,[34] S. Torre,[44] D. Torretta,[16] S. Tourneur,[16] W. Trischuk,[32] R. Tsuchiya,[55] S. Tsuno,[39] N. Turini,[44] F. Ukegawa,[53] T. Unverhau,[20] S. Uozumi,[53] D. Usynin,[43] L. Vacavant,[28] A. Vaiciulis,[47] S. Vallecorsa,[19] A. Varganov,[33] E. Vataga,[36] G. Velev,[16] G. Veramendi,[23] V. Veszpremi,[46] T. Vickey,[23] R. Vidal,[16] I. Vila,[11] R. Vilar,[11] I. Vollrath,[32] I. Volobouev,[28] F. Würthwein,[9] P. Wagner,[51] R. G. Wagner,[2] R. L. Wagner,[16] W. Wagner,[25] R. Wallny,[8] T. Walter,[25] Z. Wan,[50] M. J. Wang,[1] S. M. Wang,[17] A. Warburton,[32] B. Ward,[20] S. Waschke,[20] D. Waters,[30] T. Watts,[50] M. Weber,[28] W. C. Wester III,[16] B. Whitehouse,[54] D. Whiteson,[43] A. B. Wicklund,[2] E. Wicklund,[16] H. H. Williams,[43] P. Wilson,[16] B. L. Winer,[38] P. Wittich,[43] S. Wolbers,[16] C. Wolfe,[13] S. Worm,[50] T. Wright,[33] X. Wu,[19] S. M. Wynne,[29] A. Yagil,[16] K. Yamamoto,[40] J. Yamaoka,[50] Y. Yamashita.,[39] C. Yang,[58] U. K. Yang,[13] W. M. Yao,[28] G. P. Yeh,[16] J. Yoh,[16] K. Yorita,[13] T. Yoshida,[40] I. Yu,[27] S. S. Yu,[43] J. C. Yun,[16] L. Zanello,[49] A. Zanetti,[52] I. Zaw,[21] F. Zetti,[44] X. Zhang,[23] J. Zhou,[50] and S. Zucchelli[5]

(CDF Collaboration)

[1]*Institute of Physics, Academia Sinica, Taipei, Taiwan 11529, Republic of China*
[2]*Argonne National Laboratory, Argonne, Illinois 60439, USA*
[3]*Institut de Fisica d'Altes Energies, Universitat Autonoma de Barcelona, E-08193, Bellaterra (Barcelona), Spain*
[4]*Baylor University, Waco, Texas 76798, USA*
[5]*Istituto Nazionale di Fisica Nucleare, University of Bologna, I-40127 Bologna, Italy*
[6]*Brandeis University, Waltham, Massachusetts 02254, USA*
[7]*University of California, Davis, Davis, California 95616, USA*
[8]*University of California, Los Angeles, Los Angeles, California 90024, USA*
[9]*University of California, San Diego, La Jolla, California 92093, USA*
[10]*University of California, Santa Barbara, Santa Barbara, California 93106, USA*
[11]*Instituto de Fisica de Cantabria, CSIC-University of Cantabria, 39005 Santander, Spain*
[12]*Carnegie Mellon University, Pittsburgh, Pennsylvania 15213, USA*
[13]*Enrico Fermi Institute, University of Chicago, Chicago, Illinois 60637, USA*
[14]*Joint Institute for Nuclear Research, RU-141980 Dubna, Russia*
[15]*Duke University, Durham, North Carolina 27708, USA*
[16]*Fermi National Accelerator Laboratory, Batavia, Illinois 60510, USA*
[17]*University of Florida, Gainesville, Florida 32611, USA*
[18]*Laboratori Nazionali di Frascati, Istituto Nazionale di Fisica Nucleare, I-00044 Frascati, Italy*
[19]*University of Geneva, CH-1211 Geneva 4, Switzerland*
[20]*Glasgow University, Glasgow G12 8QQ, United Kingdom*

^{21}Harvard University, Cambridge, Massachusetts 02138, USA

^{22}Division of High Energy Physics, Department of Physics, University of Helsinki and Helsinki Institute of Physics,
FIN-00014, Helsinki, Finland

^{23}University of Illinois, Urbana, Illinois 61801, USA

^{24}The Johns Hopkins University, Baltimore, Maryland 21218, USA

^{25}Institut für Experimentelle Kernphysik, Universität Karlsruhe, 76128 Karlsruhe, Germany

^{26}High Energy Accelerator Research Organization (KEK), Tsukuba, Ibaraki 305, Japan

^{27}Center for High Energy Physics: Kyungpook National University, Taegu 702-701; Seoul National University, Seoul 151-742;
and SungKyunKwan University, Suwon 440-746, Korea

^{28}Ernest Orlando Lawrence Berkeley National Laboratory, Berkeley, California 94720, USA

^{29}University of Liverpool, Liverpool L69 7ZE, United Kingdom

^{30}University College London, London WC1E 6BT, United Kingdom

^{31}Massachusetts Institute of Technology, Cambridge, Massachusetts 02139, USA

^{32}Institute of Particle Physics: McGill University, Montréal, Canada H3A 2T8;
and University of Toronto, Toronto, Canada M5S 1A7

^{33}University of Michigan, Ann Arbor, Michigan 48109, USA

^{34}Michigan State University, East Lansing, Michigan 48824, USA

^{35}Institution for Theoretical and Experimental Physics, ITEP, Moscow 117259, Russia

^{36}University of New Mexico, Albuquerque, New Mexico 87131, USA

^{37}Northwestern University, Evanston, Illinois 60208, USA

^{38}The Ohio State University, Columbus, Ohio 43210, USA

^{39}Okayama University, Okayama 700-8530, Japan

^{40}Osaka City University, Osaka 588, Japan

^{41}University of Oxford, Oxford OX1 3RH, United Kingdom

^{42}University of Padova, Istituto Nazionale di Fisica Nucleare, Sezione di Padova-Trento, I-35131 Padova, Italy

^{43}University of Pennsylvania, Philadelphia, Pennsylvania 19104, USA

^{44}Istituto Nazionale di Fisica Nucleare Pisa, Universities of Pisa, Siena and Scuola Normale Superiore, I-56127 Pisa, Italy

^{45}University of Pittsburgh, Pittsburgh, Pennsylvania 15260, USA

^{46}Purdue University, West Lafayette, Indiana 47907, USA

^{47}University of Rochester, Rochester, New York 14627, USA

^{48}The Rockefeller University, New York, New York 10021, USA

^{49}Istituto Nazionale di Fisica Nucleare, Sezione di Roma 1, University di Roma "La Sapienza," I-00185 Roma, Italy

^{50}Rutgers University, Piscataway, New Jersey 08855, USA

^{51}Texas A&M University, College Station, Texas 77843, USA

^{52}Istituto Nazionale di Fisica Nucleare, University of Trieste/ Udine, Italy

^{53}University of Tsukuba, Tsukuba, Ibaraki 305, Japan

^{54}Tufts University, Medford, Massachusetts 02155, USA

^{55}Waseda University, Tokyo 169, Japan

^{56}Wayne State University, Detroit, Michigan 48201, USA

^{57}University of Wisconsin, Madison, Wisconsin 53706, USA

^{58}Yale University, New Haven, Connecticut 06520, USA

We report an observation of the decay $B_s^0 \rightarrow D_s^- \pi^+$ in $p\bar{p}$ collisions at $\sqrt{s} = 1.96$ TeV using 115 pb^{-1} of data collected by the CDF II detector at the Fermilab Tevatron. We observe 83 ± 11(stat) $B_s^0 \rightarrow D_s^- \pi^+$ candidates, representing a large increase in statistics over previous measurements and the first observation of this decay at a $p\bar{p}$ collider. We present the first measurement of the relative branching fraction $\mathcal{B}(B_s^0 \rightarrow D_s^- \pi^+)/\mathcal{B}(B^0 \rightarrow D^- \pi^+) = 1.32 \pm 0.18$(stat) ± 0.38(syst). We also measure $\mathcal{B}(B^+ \rightarrow \bar{D}^0 \pi^+)/\mathcal{B}(B^0 \rightarrow D^- \pi^+) = 1.97 \pm 0.10$(stat) ± 0.21(syst), which is consistent with previous measurements.

B_s^0-$\bar{B}_s^0$ oscillation is expected to occur in the standard model of particle physics. Measurement of the oscillation frequency, when combined with that for B^0-$\bar{B}^0$ oscillation, tests the unitarity of the Cabibbo-Kobayashi-Maskawa (CKM) quark mixing matrix. A deviation from unitarity could arise from a variety of new physics effects [1]. B_s^0 meson oscillations have yet to be directly observed, with a lower limit (95% C.L.) on the oscillation frequency cur-

rently at 14.5 ps^{-1} [2]. For comparison, the average B meson lifetime is of the order of 1 ps, and the B^0 oscillation frequency is 0.5 ps^{-1}. This lower limit implies that excellent proper time resolution is required to observe the oscillation. In semileptonic B_s^0 decays, the proper time measurement is degraded due to the undetected neutrino. Fully reconstructed hadronic B_s^0 decays such as $B_s^0 \rightarrow D_s^- \pi^+$ do not suffer from this problem [3]. Obtaining a

large sample of such decays is an important first step toward measuring B_s^0 mixing.

In addition, the measurement of the branching ratio of $B_s^0 \to D_s^- \pi^+$ decay along with that of $B^0 \to D^- \pi^+$ and $B^+ \to \bar{D}^0 \pi^+$ can be used to study B meson decay mechanisms. As shown in Fig. 1, $B_s^0 \to D_s^- \pi^+$ decay proceeds only at tree level while the B^0 and B^+ modes have additional, nontree, contributions. Therefore, measurements of ratios of branching fractions of these decays can, in principle, isolate contributions from the different decay diagrams [4].

To date, a few $B_s^0 \to D_s^- \pi^+$ events have been observed [5,6] in $e^+ e^-$ collisions at LEP. B factories, while running at the $\Upsilon(4S)$ resonance, do not produce B_s^0 mesons. However, large samples of B_s^0 are produced at the Tevatron. The ability to trigger on displaced vertices allows the upgraded collider detector at Fermilab (CDF II) to collect large samples of fully reconstructed B_s^0 decay modes.

In this Letter, we present an observation of $B_s^0 \to D_s^- \pi^+$ decays and a measurement of the ratios of branching fractions of $B_s^0 \to D_s^- \pi^+$ and $B^+ \to \bar{D}^0 \pi^+$ relative to the branching fraction of $B^0 \to D^- \pi^+$ decays. We use a sample of fully reconstructed $B \to D\pi$ decays corresponding to 115 pb^{-1} of $p\bar{p}$ collisions at $\sqrt{s} = 1.96$ TeV collected by the CDF II detector at the Fermilab Tevatron between February 2002 and January 2003. Charge conjugate modes are implied throughout this Letter.

The components of the CDF II detector relevant to this analysis are described briefly below; a more complete description can be found elsewhere [7]. We use tracks reconstructed by both the central outer tracker (COT) and the silicon microstrip detector (SVX II) in the range $|\eta| \leq 1$ [8], where η is the pseudorapidity defined as $\eta = -\ln\tan(\theta/2)$ and θ is the polar angle with respect to the proton beam direction. The SVX II detector consists of double-sided silicon strip sensors arranged in five cylindrical shells with radii between 2.5 and 10.6 cm [9]. Surrounding the SVX II is the COT [10], an open-cell drift chamber that has an inner (outer) radius of 40 (137) cm. The COT has 96 layers, organized in 8 superlayers with alternating superlayers of axial and $\pm 2°$ stereo readout. The B decays used in this analysis are selected with a three-level trigger system. At Level 1, charged tracks are reconstructed in the COT axial superlayers by a hardware processor, the eXtremely fast tracker (XFT) [11]. This trigger
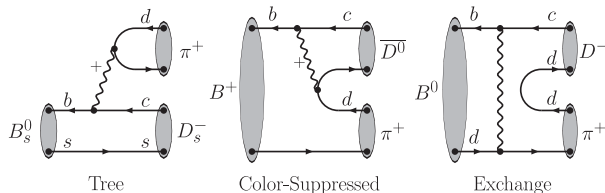
requires two oppositely charged tracks with transverse momenta $p_T \gtrsim 2$ GeV/c and scalar sum $p_{T1} + p_{T2} \gtrsim 5.5$ GeV/c. At Level 2, the silicon vertex trigger (SVT) [12] associates SVX II $r - \varphi$ position measurements with XFT tracks. This provides a precise measurement of the track impact parameter, d_0, which is defined as the projection of a track's distance of closest approach to the beam line onto the transverse plane. The resolution of the impact parameter measurement is 50 μm, which includes approximately 30 μm contribution from the transverse beam size. Hadronic decays of heavy flavor particles are selected by requiring two tracks with 120 μm $\leq d_0 \leq$ 1000 μm. The two trigger tracks must have an opening angle in the transverse plane satisfying $2° \leq |\Delta\varphi| \leq 90°$ and must satisfy the requirement $L_{xy} > 200$ μm, where L_{xy} is defined as the distance in the transverse plane from the beam line to the two-track vertex projected onto the two-track momentum vector. A complete event reconstruction is performed at Level 3, and the Level 1 and Level 2 requirements are confirmed. Since events satisfying the displaced vertex trigger are dominated by the decays of promptly produced charm, the largest background to $B \to D\pi$ decays results from combining a prompt D meson with an unrelated track from the event.

Reconstruction of B meson candidates begins by selecting D meson candidates. We reconstruct the following D meson decay modes: $\bar{D}^0 \to K^+ \pi^-$, $D^- \to K^+ \pi^- \pi^-$ and $D_s^- \to \phi\pi^-$ followed by $\phi \to K^+ K^-$. We exploit the narrow $\phi \to K^+ K^-$ resonance in the D_s^- decays to greatly suppress background by requiring 1010 MeV/c^2 < $m(K^+ K^-)$ < 1028 MeV/c^2. No particle identification is used in this analysis. All particle hypotheses consistent with the candidate decay structure are attempted. The track combinations which comprise a D meson candidate are required to originate from a common vertex. An additional track with $p_T > 1.6$ GeV/c and $\Delta R(D, \pi_B) < 1.5$ is added and assigned a pion mass to reconstruct the B meson candidate. We define $\Delta R = \sqrt{\Delta\eta^2 + \Delta\varphi^2}$, where $\Delta\varphi$ and $\Delta\eta$ are the azimuthal angle and pseudorapidity of the pion with respect to the direction of the D meson candidate. The selection requirements are optimized to yield the largest $S/\sqrt{S + B}$ for each of the decays. In the optimization procedure, the number of signal events (S) is estimated using a Monte Carlo simulation, while the number of background events (B) is estimated using sidebands of the B meson mass spectra reconstructed in data.

We require the B meson candidate tracks to be consistent with the following constraints: the D meson tracks originate from a common vertex, the momentum of the D meson points back, in three dimensions, to the remaining B meson candidate track, and the invariant mass of the D meson decay products is consistent with the world average of the corresponding D meson mass [2]. We also require that at least two of the B meson daughter tracks are consistent with the trigger requirements. The combinatorial

FIG. 1.   Different Feynman diagrams which contribute to $B \to D\pi$ decays.

background is strongly reduced by requiring that $L_{xy}^B >$ 400 μm and $L_{xy}(B \to D) > -150$ μm, where the latter refers to the L_{xy} of the D meson decay vertex with respect to the B meson decay vertex. The impact parameter of the B meson momentum with respect to the beam axis is required to be less than 80 μm to assure that the B meson candidate originates from the primary vertex. The invariant mass distributions of B_s^0, B^+, and B^0 meson candidates are shown in Fig. 2. The prominent peak at each expected B meson mass establishes $B \to D\pi$ decay signals, including our observation of $B_s^0 \to D_s^- \pi^+$.

We measure the following ratio:

$$\frac{\mathcal{B}(B_s^0 \to D_s^- \pi^+)}{\mathcal{B}(B^0 \to D^- \pi^+)} = \frac{N(B_s^0)}{N(B^0)} \frac{\epsilon(B^0)}{\epsilon(B_s^0)} \frac{f_d}{f_s}$$
$$\times \frac{\mathcal{B}(D^- \to K^+ \pi^- \pi^-)}{\mathcal{B}(D_s^- \to \phi \pi^-)\mathcal{B}(\phi \to K^+ K^-)}$$
(1)

where $N(B_s^0)$ and $N(B^0)$ are the signal yields, f_d/f_s is the ratio of fragmentation fractions for B^0 and B_s^0 mesons, and $\epsilon(B^0)/\epsilon(B_s^0)$ is the ratio of trigger and reconstruction efficiencies. Equation (1) also applies to the $B^+ \to \bar{D}^0 \pi^+$ mode, with terms for B_s^0 decays replaced by those relevant
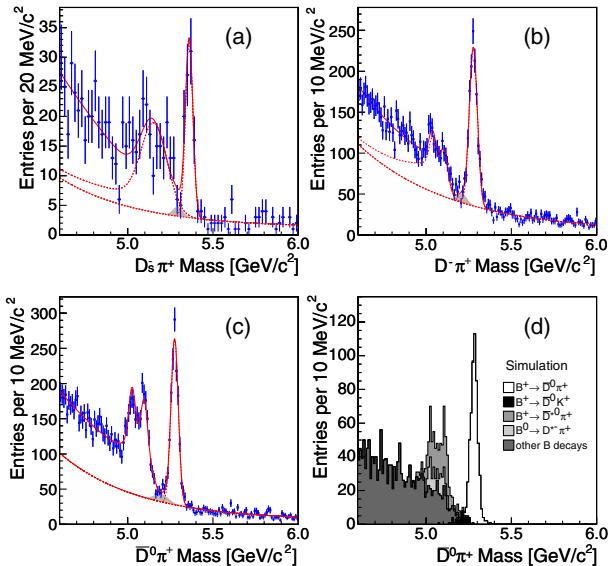

FIG. 2 (color online).   Invariant mass spectra for (a) $D_s^- \pi^+$, (b) $D^- \pi^+$, and (c) $\bar{D}^0 \pi^+$ for data, with χ^2 fits overlaid. The main background under the signal peak is combinatorial, modeled with a combination of a linear and exponential function. The shaded peak corresponds to $B \to DK$ decays, and is modeled with a Gaussian. The additional background component in the low mass region is due to partially reconstructed B decays. This background component is modeled using shapes determined by inclusive $B \to DX$ Monte Carlo simulations. A sample Monte Carlo mass distribution for $B^+ \to \bar{D}^0 \pi^+$ events is shown in (d). Contributions from different sources in (d) are ordered by peak position, from right to left.

to B^+ decays. There are three components to the ratio of branching fractions measurement: the ratio of B meson yields obtained from fits to the invariant mass spectra, the ratio of signal efficiencies obtained from Monte Carlo simulation, and the product of previously measured production and branching fractions.

In our analysis, we use Monte Carlo simulation to determine shapes of mass spectra and relative efficiencies. The Monte Carlo generation proceeds as follows. Transverse momentum and rapidity distributions of single b quarks are generated based on calculations using next-to-leading-order perturbative QCD [13]. B meson kinematic distributions are obtained by simulating Peterson fragmentation [14] on quark-level distributions. Additional fragmentation particles, correlated b-$\bar{b}$ production and the underlying event structure are not simulated. B meson decays are simulated using EvtGen [15]. The simulation of the CDF II detector and trigger is based upon a GEANT 3 description [16] that includes effects of time variation of the beam position and hardware configuration of the SVX II and SVT.

The yield of B mesons is extracted from the invariant mass spectra using a binned χ^2 fit, as shown in Fig. 2. There are three contributions to the background shape used in the fit. The combinatorial background component is modeled with a linear combination of a linear and exponential distribution. The shape of background due to Cabibbo-suppressed $B \to DK$ decay is modeled by a Gaussian and is shown as shaded distributions in Figs. 2(a)–2(c). Backgrounds due to partially reconstructed B decays contribute to the low mass side of the signal peak and are modeled by inclusive $B \to DX$ Monte Carlo simulation. The structures in the region close to the signal are due to $B \to D^* \pi$ decays, where a photon or a π^0 from the D^* decay is not reconstructed. The decay of the polarized D^* produces the double-peaked structure. As an example of the various contributing backgrounds, Fig. 2(d) shows the invariant mass spectrum for $B \to DX$ Monte Carlo reconstructed as $B^+ \to \bar{D}^0 \pi^+$. In the fit to the data mass spectrum, the fractions of combinatorial background and partially reconstructed B's are allowed to float in the fit. The ratio of Cabibbo-suppressed $B \to DK$ background to the corresponding signal is fixed to the world average ratio of branching fractions, with the trigger and reconstruction efficiencies of the two modes taken into account. The fitted yields of $B^0 \to D^- \pi^+$, $B^+ \to \bar{D}^0 \pi^+$, and $B_s^0 \to D_s^- \pi^+$ decays are 1118 ± 43(stat), 1260 ± 42(stat) and 83 ± 11(stat) events, respectively.

Trigger and reconstruction efficiencies for B^0, B^+, and B_s^0 decays are determined using Monte Carlo simulation. The trigger efficiency differs among the three B meson decay modes due to differences in decay kinematics (e.g., opening angle distributions) which arise from the different masses and spins of the intermediate and final state particles. The ratios of efficiencies are

$\epsilon(B^0)/\epsilon(B^+) = 0.708 \pm 0.010$　　and　　$\epsilon(B^0)/\epsilon(B^0_s) = 0.903 \pm 0.012$, where the uncertainties are due to the limited statistics of Monte Carlo samples.

World average values [2] are used for the various branching fractions in Eq. (1). In terms of B meson production, we assume $f_d = f_u$, consistent with previous measurement [17]. The B^0_s/B^0 production fraction used in this analysis is the world average value, $f_s/f_d = 0.270 \pm 0.029$, currently dominated by LEP measurements. The ratio of fragmentation fractions may be different in a hadron collider environment than in $e^+ e^-$ collisons. However, the ratio of fragmentation fractions measured by CDF [17] is consistent with the LEP results.

Many systematic uncertainties cancel in the measurement of ratios of branching fractions due to the similarity of final state kinematics. Systematic uncertainties come from three main sources: fitting the invariant mass distributions to obtain signal yields, determination of the ratio of efficiencies, and uncertainties on external inputs. The contribution to the systematic uncertainty from externally measured quantities is calculated by propagating world average uncertainties. Systematic uncertainties on the signal yields are determined by comparing the fitted yields after changing the invariant mass region of the fit and varying the background shape within the range allowed by the $B \rightarrow DX$ Monte Carlo statistics and world average uncertainties on the branching fractions of participating B decays. Systematic uncertainties on the ratio of efficiencies come from physics sources such as the choice of p_T spectrum or meson lifetime, and detector sources such as inaccuracies in the XFT and SVT hardware simulation. The uncertainty due to a given source is estimated by the shift of the ratio of efficiencies when the effect of that source is modified in the Monte Carlo simulation. The effect of the choice of B meson p_T spectrum is estimated by reweighting the Monte Carlo simulation to match the measured B hadron p_T spectrum [7]. Since the trigger and

analysis selection only accept events in which the B meson is displaced from the primary interaction point, the efficiencies depend upon the B and D meson lifetimes. To estimate uncertainties due to B and D meson lifetimes, the Monte Carlo simulation is reweighted with different lifetimes within the world average uncertainties. Because of the different specific ionization of $\pi^\pm$ and $K^\pm$ in the COT, kaons are 6% less efficient in satisfying the XFT requirements [18]. The Monte Carlo simulation is reweighted to reproduce this effect. To estimate the uncertainty due to imperfections in simulating the signal selection requirement efficiencies, we compare efficiencies between Monte Carlo simulation and sideband subtracted B^+ and B^0 signal for every selection requirement separately. In the case of the B^+/B^0 branching fraction ratio measurement, there is an additional systematic uncertainty associated with the fact that the B^0 decay has four tracks in the final state while B^+ has only three. We infer the corrections and systematic uncertainties due to the fourth track by comparing trigger and reconstruction efficiencies in data and Monte Carlo simulations for semileptonic $B \rightarrow D^{*-} l^+ X, D^{*-} \rightarrow \bar{D}^0 \pi^-$ decays between the $\bar{D}^0 \rightarrow K^+ \pi^-$ and $K^+ \pi^- \pi^+ \pi^-$ final states.

The systematic uncertainties are summarized in Table I. The total systematic uncertainty is obtained by adding individual contributions in quadrature. Using Eq. (1), we obtain the following values for the ratios of branching fractions:

$$\frac{\mathcal{B}(B^0_s \rightarrow D^-_s \pi^+)}{\mathcal{B}(B^0 \rightarrow D^- \pi^+)} = 1.32 \pm 0.18(\text{stat}) \pm 0.10(\text{syst})$$
$$\pm 0.34(\text{BR}) \pm 0.14(\text{PR}), \qquad (2)$$

$$\frac{\mathcal{B}(B^+ \rightarrow \bar{D}^0 \pi^+)}{\mathcal{B}(B^0 \rightarrow D^- \pi^+)} = 1.97 \pm 0.10(\text{stat}) \pm 0.15(\text{syst})$$
$$\pm 0.14(\text{BR}), \qquad (3)$$

where BR and PR refer to the uncertainty on the ratio of D meson branching fractions and B^0_s meson production relative to B^0, respectively. Under the assumption of isospin invariance, our measurement of the ratio $\mathcal{B}(B^+ \rightarrow \bar{D}^0 \pi^+)/\mathcal{B}(B^0 \rightarrow D^- \pi^+)$ is consistent with the world average [2]. This provides a high statistics cross-check of the measurement procedure.

In conclusion, we have presented the first observation of $B^0_s \rightarrow D^-_s \pi^+$ decays in $p\bar{p}$ collisions, and the first measurement of the $B^0_s \rightarrow D^-_s \pi^+$ branching fraction relative to the $B^0 \rightarrow D^- \pi^+$ branching fraction. The precision of this measurement is currently not adequate to separate the contributions of different decay diagrams [4]. We expect the measurement precision to improve as world average values of D meson branching fractions and B meson production fractions improve.

TABLE I.　Summary of relative systematic uncertainties.

Effect	B^0_s/B^0 [%]	B^+/B^0 [%]
fit $N(B^0_s, B^+)$	4.5	2.0
fit $N(B^0)$	2.3	2.3
B_{p_T} spectrum	2.6	1.5
trigger simulation	1.6	0.2
selection simulation	4.0	4.0
ϕ^0 mass cut	0.2	not applicable
B^+/B^0_s meson lifetime	2.0	0.4
D^0/D^-_s meson lifetime	0.1	0.1
B^0 meson lifetime	0.4	0.4
D^- meson lifetime	<0.1	<0.1
fourth track accept	not applicable	5.2
Total	7.4	7.4

[1] A. J. Buras *et al.*, Phys. Lett. B **500**, 161 (2001).

[2] S. Eidelman *et al.*, Phys. Lett. B **592**, 1 (2004).

[3] K. Anikeev *et al.*, Fermilab Report No. FERMILAB-PUB-01-197 (2001).

[4] A. K. Leibovich, Z. Ligeti, I. W. Stewart, and M. B. Wise, Phys. Lett. B **586**, 337 (2004).

[5] D. Buskulic *et al.* (ALEPH Collaboration), Phys. Lett. B **311**, 425 (1993).

[6] R. Akers *et al.* (OPAL Collaboration), Phys. Lett. B **337**, 196 (1994).

[7] D. Acosta *et al.* (CDF Collaboration), Phys. Rev. D **71**, 032001 (2005).

[8] CDF II uses a cylindrical coordinate system in which φ is the azimuthal angle, r is the radius from the nominal beamline, y points up, and z points in the proton beam direction with the origin at the center of the detector. The transverse plane is the plane perpendicular to the z axis. A superconducting magnet provides a nearly uniform 1.4 T axial field in which charged particles are reconstructed.

[9] A. Sill *et al.*, Nucl. Instrum. Methods Phys. Res., Sect. A **447**, 1 (2000).

[10] T. Affolder *et al.*, Nucl. Instrum. Methods Phys. Res., Sect. A **526**, 249 (2004).

[11] E. J. Thomson *et al.*, IEEE Trans. Nucl. Sci. **49**, 1063 (2002).

[12] W. Ashmanskas *et al.*, Nucl. Instrum. Methods Phys. Res., Sect. A **518**, 532 (2004).

[13] P. Nason, S. Dawson, and R. K. Ellis, Nucl. Phys. **B303**, 607 (1988).

[14] C. Peterson, D. Schlatter, I. Schmitt, and P. M. Zerwas, Phys. Rev. D **27**, 105 (1983).

[15] D. J. Lange, Nucl. Instrum. Methods Phys. Res., Sect. A **462**, 152 (2001).

[16] R. Brun, R. Hagelberg, M. Hansroul, and J. C. Lassalle, CERN Reports No. CERN-DD-78-2-REV and No. CERN-DD-78-2.

[17] T. Affolder *et al.* (CDF Collaboration), Phys. Rev. Lett. **84**, 1663 (2000).

[18] D. Acosta *et al.* (CDF Collaboration), Phys. Rev. Lett. **94**, 122001 (2005).